Relativistic laser-plasma interactions in the quantum regime

Bengt Eliasson[1] and P. K. Shukla[2]

[1]*Institut für Theoretische Physik, Fakultät für Physik und Astronomie, Ruhr-Universität Bochum, D-44780 Bochum, Germany*

[2]*RUB International Chair, International Centre for Advanced Studies in Physical Sciences, Fakultät für Physik und Astronomie, Ruhr-Universität Bochum, D-44780 Bochum, Germany*

(Received 14 October 2010; revised manuscript received 16 February 2011; published 21 April 2011)

We consider nonlinear interactions between a relativistically strong laser beam and a plasma in the quantum regime. The collective behavior of electrons is modeled by a Klein-Gordon equation, which is nonlinearly coupled with the electromagnetic wave through the Maxwell and Poisson equations. This allows us to study nonlinear interactions between arbitrarily large-amplitude electromagnetic waves and a quantum plasma. We have used our system of nonlinear equations to study theoretically the parametric instabilities involving stimulated Raman scattering and modulational instabilities. A model for quasi-steady-state propagating electromagnetic wave packets is also derived, and which shows possibility of localized solitary structures in a quantum plasma. Numerical simulations demonstrate collapse and acceleration of electrons in the nonlinear stage of the modulational instability, as well as possibility of the wake-field acceleration of electrons to relativistic speeds by short laser pulses at nanometer length scales. Our study is relevant for understanding the localization of intense electromagnetic pulses in a quantum plasma with extremely high electron densities and relatively low temperature.

DOI: 10.1103/PhysRevE.83.046407 PACS number(s): 52.35.Mw, 52.38.Hb, 52.40.Db

I. INTRODUCTION

With the advent of the x-ray free-electron lasers [1] there are new possibilities for exploring matter on atomic and single-molecule levels. On these length scales, of the order of a few angstroms, quantum effects play an important role in the dynamics of the electrons. Quantum effects have been measured experimentally both in the degenerate electron gas in metals and in warm dense matters [2]. It has also been found that quantum mechanical effects must be taken into account in intense laser-solid density plasma interaction experiments [3–5]. Nonlinear interactions of large-amplitude electromagnetic (EM) waves with the plasma can lead to various parametric instabilities [6–8]. At laser intensities around 10^{19} W/cm^2 and above, nonlinearity associated with relativistic electron mass increase in short laser pulses plays a significant role. Furthermore, the relativistic ponderomotive force [9] of intense laser pulses produces density modifications. Thus, in a classical plasma, nonlinear effects associated with relativistic electron mass increase and relativistic ponderomotive force are very important, since they provide possibility of the modulational instability [10,11] followed by a compression and localization of intense EM waves. In addition to the modulational instability, there are relativistic Raman forward and backward scattering instabilities [12–15] and the two-plasmon decay [16] instability that lead to strong collisionless heating of the plasma in the relativistic regime. The parametric instabilities of intense EM waves in a magnetized plasma have also been investigated [17–19].

However, for intense EM waves interacting with the plasma in the x-ray and γ-ray regimes, both relativistic and quantum effects must be taken into account on an equal footing. Accordingly, in this paper, we present a simplified nonlinear model, based on the Klein-Gordon (KG) equation coupled with the Maxwell equations that are capable of treating both the relativistic (propagation and mass increase) and quantum (tunneling or diffraction) effects, but neglects electron spin effects. The latter can be motivated by the fact that the main source of nonlinear interactions between the EM waves and the plasma is via the ponderomotive force, while the electron spin-1/2 effect comes in as a perturbation. Similar models have been discussed in the past by Takabayasi [20] and, using the Feshbach-Villars Hamiltonian formalism for a bosonic gas [21], by Hines and Frankel [22] and Kowalenko *et al*. [23]. Previous investigations have focused on the general formulation of quantum mechanics and on linear eigenmodes in a quantum plasma; here we will use the basic model to investigate the nonlinear coupling between large-amplitude EM waves and electrostatic oscillations and structures. Our work has potential applications in laser-matter experiments [2,24], quantum free-electron laser systems [25–27], as well as in astrophysical environments [28–30].

The manuscript is organized as follows. In Sec. II, we present our mathematical model for the coupled KG and Maxwell equations, exhibiting nonlinear interactions between relativistic electrons and EM fields. Linear properties of the electrostatic waves are discussed in Sec. III. Section IV shows how our governing equations lead to the wave equation that reveals the phenomena of relativistic nonlinear propagation and self-induced transparency of EM waves. Section V is concerned with the theoretical and numerical investigations of the relativistic parametric instabilities in the quantum regime. Section VI deals with relativistic optical solitary waves. The nonlinear dynamics of interacting intense localized EM pulses, as well as the new phenomena of the formation of nonlinear Bernstein-Greene-Krushkal (BGK) -like modes and associated electron acceleration, are described in Sec. VII. Section VIII contains a brief summary and conclusions.

II. MATHEMATICAL MODEL

Historically, the Klein-Gordon equation (KGE) for an electron is obtained from the relativistic relation between the

energy $\mathcal{E}$ and the momentum $\mathbf{p}$, namely,

$$\mathcal{E}^2 = \mathbf{p}^2c^2 + m_e^2c^4, \tag{1}$$

where c is the speed of light in vacuum and m_e the electron mass. By the substitution $\mathcal{E} \to i\hbar\partial/\partial t$ and $\mathbf{p} \to -i\hbar\nabla$ in (1), where $\hbar$ is the Planck constant divided by 2π, we obtain the KGE for a free electron as

$$\hbar^2\frac{\partial^2\psi}{\partial t^2} - \hbar^2c^2\nabla^2\psi + m_e^2c^4\psi = 0, \tag{2}$$

where ψ is the electron wavefunction. The free-particle KGE fulfills the continuity equation

$$\frac{\partial\rho_e}{\partial t} + \nabla\cdot\mathbf{j}_e = 0, \tag{3}$$

where

$$\rho_e = -\frac{ie\hbar}{2m_ec^2}\left(\psi^*\frac{\partial\psi}{\partial t} - \psi\frac{\partial\psi^*}{\partial t}\right), \tag{4}$$

and

$$\mathbf{j}_e = \frac{ie\hbar}{2m_e}(\psi^*\nabla\psi - \psi\nabla\psi^*). \tag{5}$$

We have multiplied the right-hand sides of Eqs. (4) and (5) by the electron charge $-e$, so that ρ_e can be interpreted as the electric charge density and $\mathbf{j}$ as the electric current density. Since ρ_e is neither positive nor negative definite, it cannot be interpreted as a probability density; however, it can be interpreted as a charge density that need not have a definite sign.

We now wish to use the charge and current densities as sources for the self-consistent EM scalar and vector potentials ϕ and $\mathbf{A}$ for a quantum plasma [20], so that ψ represents an ensemble of charged electrons. Introducing the EM potentials into the KGE, we make the usual substitutions $i\hbar\partial/\partial t \to i\hbar\partial/\partial t + e\phi$ and $-i\hbar\nabla \to -i\hbar\nabla + e\mathbf{A}$, and obtain

$$\mathcal{W}^2\psi - c^2\mathcal{P}^2\psi - m_e^2c^4\psi = 0, \tag{6}$$

where we have defined the energy and momentum operators as

$$\mathcal{W} = i\hbar\frac{\partial}{\partial t} + e\phi, \tag{7}$$

and

$$\mathcal{P} = -i\hbar\nabla + e\mathbf{A}, \tag{8}$$

respectively. The electric charge and current densities are now obtained as

$$\rho_e = -\frac{e}{2m_ec^2}[\psi^*\mathcal{W}\psi + \psi(\mathcal{W}\psi)^*] \tag{9}$$

and

$$\mathbf{j}_e = -\frac{e}{2m_e}[\psi^*\mathcal{P}\psi + \psi(\mathcal{P}\psi)^*], \tag{10}$$

respectively, and in this form they fulfill the continuity equation (3).

The self-consistent vector and scalar potentials are obtained from the EM wave equations

$$\frac{\partial^2\mathbf{A}}{\partial t^2} + c^2\nabla\times(\nabla\times\mathbf{A}) + \nabla\frac{\partial\phi}{\partial t} = \mu_0c^2\mathbf{j}_e \tag{11}$$

and

$$\nabla^2\phi + \nabla\cdot\frac{\partial\mathbf{A}}{\partial t} = -\frac{1}{\varepsilon_0}(\rho_e + \rho_i), \tag{12}$$

where μ_0 is the magnetic vacuum permeability and ε_0 is the electric permittivity in a vacuum, and ρ_i is the neutralizing positive charge density due to the ions. For immobile, singly charged ions, one can assume that $\rho_i = en_0$, where n_0 is the equilibrium ion number density. The assumption of immobile ions is justified because we are studying nonlinear phenomena on a timescale much shorter than the ion plasma period.

Using the Coulomb gauge $\nabla\cdot\mathbf{A} = 0$, we obtain from Eqs. (11) and (12)

$$\frac{\partial^2\mathbf{A}}{\partial t^2} - c^2\nabla^2\mathbf{A} + \nabla\frac{\partial\phi}{\partial t} = \mu_0c^2\mathbf{j}_e \tag{13}$$

and

$$\nabla^2\phi = -\frac{1}{\varepsilon_0}(\rho_e + \rho_i), \tag{14}$$

respectively. Taking the divergence of both sides of Eq. (13), we have

$$\nabla^2\frac{\partial\phi}{\partial t} = \mu_0c^2\nabla\cdot\mathbf{j}_e, \tag{15}$$

so that Eq. (13) can be written as

$$\nabla^2\left(\frac{\partial^2\mathbf{A}}{\partial t^2} - c^2\nabla^2\mathbf{A}\right) = -\mu_0c^2\nabla\times(\nabla\times\mathbf{j}_e). \tag{16}$$

Equations (6), (14), and (16) are our desired system that describes nonlinear interactions between intense laser beams and an unmagnetized plasma in the quantum regime. We note that the KGE, given by Eq. (6), is valid for relativistic electrons without the spin-1/2 effect. The latter could be important in a magnetized quantum plasma where one should also account for the electron spin-1/2 dynamics [31–33].

The nonrelativistic limit is obtained from Eq. (6) by substituting $\psi = \Psi\exp(-im_ec^2t/\hbar)$, and by using the condition $|\hbar\partial\Psi/\partial t| \ll m_ec^2\Psi$, together with the normalization of Ψ such that $\Psi\Psi^* = n_0$ is the electron number density at the equilibrium. In this limit, Eq. (6) yields the Schrödinger equation

$$i\hbar\frac{\partial\Psi}{\partial t} + \frac{1}{2m_e}(-i\hbar\nabla + e\mathbf{A})^2\Psi + e\phi\Psi = 0. \tag{17}$$

Here, and in what follows, we have used a simplified model and neglected the electron degeneracy pressure. The latter is important in dense matters where the electron degeneracy pressure appears due to the Pauli exclusion principle. For a nonrelativistic plasma, the quantum statistical pressure has been introduced in a nonlinear Schrödinger model [34], but this has to be investigated for relativistic quantum plasmas.

III. COLLECTIVE ELECTROSTATIC OSCILLATIONS AND FREE PARTICLES

In the absence of the EM field (namely, $\mathbf{A} = 0$), we still have electrostatic (ES) waves due to the charge separation between the electrons and ions. At short wavelengths, the quantum effects become important and give rise to dispersion effects in the ES wave. At these wavelengths, there is an

interplay between collective electron oscillations and free electron motion. When the wavelength is comparable to the Compton wavelength, the electrons become relativistic, and there are relativistic corrections to the dispersion relation for the electrostatic wave.

In the derivation of the dispersion relation for relativistic electrons, it is convenient to first make the transformation $\psi = \widetilde{\psi}\exp(-im_e c^2 t/\hbar)$, where the wavefunction $\widetilde{\psi}$ obeys the wave equation

$$\left(i\hbar\frac{\partial}{\partial t} + m_e c^2 + e\phi\right)^2 \widetilde{\psi} + \hbar^2 c^2 \nabla^2 \widetilde{\psi} - m_e^2 c^4 \widetilde{\psi} = 0, \quad (18)$$

and the electron charge density is

$$\rho_e = -\frac{i\hbar e}{2m_e c^2}\left(\widetilde{\psi}^*\frac{\partial\widetilde{\psi}}{\partial t} - \widetilde{\psi}\frac{\partial\widetilde{\psi}^*}{\partial t}\right) - \left(1 + \frac{e\phi}{m_e c^2}\right) e|\widetilde{\psi}|^2. \quad (19)$$

We next linearize the system (15), (19), and (20) by setting $\phi = \phi_1$ and $\widetilde{\psi} = \widetilde{\psi}_0 + \widetilde{\psi}_1$, where $\phi_1 = \widehat{\phi}\exp(i\mathbf{K}\cdot\mathbf{r} - i\Omega t)$ + complex conjugate, $\widetilde{\psi}_1 = \widehat{\psi}_+\exp(i\mathbf{K}\cdot\mathbf{r} - i\Omega t) + \widehat{\psi}_-\exp(-i\mathbf{K}\cdot\mathbf{r} + i\Omega t)$, and where $|\widetilde{\psi}_0|^2 = n_0$. Separating different Fourier modes, we obtain from (18) the dispersion relation for the ES oscillations as $\mathcal{E} = 1 + \chi_e = 0$, where $\mathcal{E}$ is the dielectric constant and the electron susceptibility is

$$\chi_e = \frac{\omega_{pe}^2\left[4m_e^2c^4 - \hbar^2(\Omega^2 - c^2K^2)\right]}{\hbar^2(\Omega^2 - c^2K^2)^2 - 4m_e^2c^4\Omega^2}, \quad (20)$$

where $\omega_{pe} = (n_0 e^2/\varepsilon_0 m_e)^{1/2}$ is the electron plasma frequency. We note that in the classical limit $\hbar \to 0$, we have $\chi_e = -\omega_{pe}^2/\Omega^2$, while in the nonrelativistic limit $c \to \infty$, we have $\chi_e = -\omega_{pe}^2/(\Omega^2 - \hbar^2k^4/4m_e^2)$. After some reordering of terms, the dispersion relation can be written as

$$\hbar^2(\Omega^2 - c^2K^2)\left(\Omega^2 - c^2K^2 - \omega_{pe}^2\right) - 4m_e^2c^4\left(\Omega^2 - \omega_{pe}^2\right) = 0. \quad (21)$$

Similar results have been obtained previously for a relativistic bosonic gas [22,23]. It is interesting to investigate some limiting cases of Eq. (21). For $\omega_{pe} \to 0$, we obtain the four solutions

$$\Omega = \mp\frac{m_e c^2}{\hbar} \pm \sqrt{\frac{m_e^2c^4}{\hbar^2} + c^2K^2}, \quad (22)$$

Choosing the upper sign (−) in front of the first term in the right-hand side of Eq. (22), we obtain the free particle solutions of the Klein-Gordon equation, where the upper sign (+) in the second term corresponds to the motion of a free electron and the negative sign (−) corresponds to a negative energy state solution, which can be interpreted as the motion of a free positron. The other two solutions (with a plus sign in front of the first term) are connected to plasma modes, which are not easy to interpret in terms of free particle solutions. In the classical limit $\hbar \to 0$, we obtain from Eq. (21) the Langmuir oscillations $\Omega = \omega_{pe}$, while in the limit $c \to \infty$, we have the nonrelativistic result

$$\Omega^2 = \omega_{pe}^2 + \frac{\hbar^2K^4}{4m_e^2}. \quad (23)$$

On the other hand, in the limit $K \to 0$, Eq. (21) yields the Langmuir (plasmon) oscillations at the plasma frequency, $\Omega = \omega_{pe}$, and the pair branch with the frequency $\Omega = 2m_e c^2/\hbar$ [23].

We note that there is a nondimensional quantum parameter

$$H = \hbar\omega_{pe}/m_e c^2 \quad (24)$$

in Eq. (21) that determines the relative importance of the quantum effect. Typical values are $H = 10^{-4}$ for the electron number density $n_e \sim 10^{30}$ m^{-3} in solid density laser-plasma experiments, and $H = 0.007$ may be representative of modern laser-compressed matter experiments with $n_e \sim 10^{34}$ m^{-3}. This corresponds to $\omega_{pe} = 8 \times 10^{16}$ s^{-1} and $\lambda_e = 4 \times 10^{-9}$ m for $H = 10^{-4}$, and $\omega_{pe} = 5.4 \times 10^{18}$ s^{-1} and $\lambda_e = 5.5 \times 10^{-11}$ m for $H = 0.007$, where $\lambda_e = c/\omega_{pe}$ is the electron skin depth. The nonrelativistic result (23) is valid for the ES waves with wavenumbers in the range $1 < K\lambda_e < 1/H$. For $K\lambda_e < 1$, the quantum corrections to $\omega \approx \omega_{pe}$ are different from (23) and turn the wave frequency slightly lower than ω_{pe} [22]. However, this effect is negligible for small values of H and may be smaller than the degeneracy electron pressure effect, which has been neglected here. On the other hand, the limit $K\lambda_e > 1/H$ corresponds to relativistic particles with $K > 1/\lambda_C$, where $\lambda_C = \hbar/m_e c \approx 3.9 \times 10^{-13}$ m is the reduced Compton wavelength.

In Fig. 1 we have plotted the solutions of the dispersion relation (21) for $H = 10^{-4}$ and 0.007. Both the electron plasma oscillations and the pair branches (positronic states) are shown. The electron plasma oscillations have a cutoff frequency $\omega \to \omega_{pe}$ when $K \to 0$, while the positronic states have a cutoff frequency $\omega \to 2m_e c^2/\hbar$, corresponding to $\omega/\omega_{pe} \to 1/H$ at $K \to 0$ in Fig. 1. For the electron plasma oscillations, the increase in the wave frequency due to the quantum effect becomes noticeable when $K\lambda_e = 1/\sqrt{H}$, or $K \approx (4\pi n_0/a_B)^{1/4}$, where $a_B = 4\pi\varepsilon_0\hbar^2/m_e e^2 \approx 5.3 \times 10^{-11}$ m is the Bohr radius. This corresponds to a wavelength of

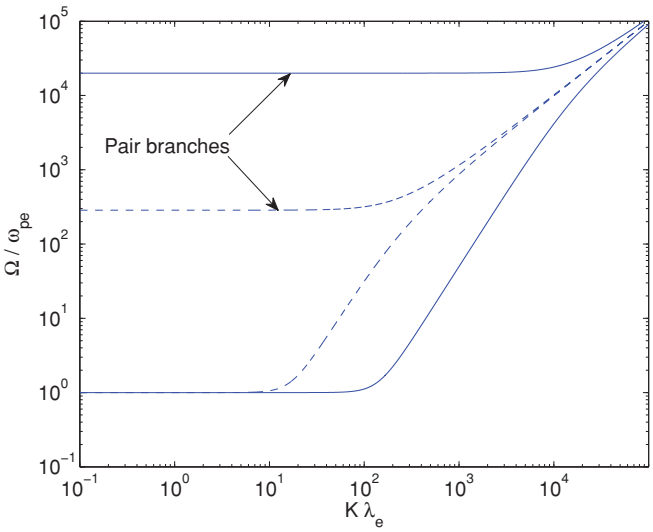

FIG. 1. (Color online) Dispersion curves (Ω vs. K) for the ES oscillations for $H = 10^{-4}$ (solid curves) and $H = 0.007$ (dashed curves), where $H = \hbar\omega_{pe}/m_e c^2$. For $K\lambda_e > 1/H$, the particle motion turns from weakly relativistic to ultrarelativistic.

$2\pi/K \approx 2.8 \times 10^{-10}$ m for $H = 10^{-4}$ and $2\pi/K \approx 5 \times 10^{-11}$ m for $H = 0.007$.

The pair branches are associated with, for example, the *Zitterbewegung* effect [35,36], in which the interference between the positive and negative energy states are predicted to give oscillations on Compton wavelength scales. The *Zitterbewegung* effect was originally predicted for Dirac particles with spin-1/2, but is also predicted in the framework of the Klein-Gordon equation for spinless particles [35]. It shall be noted that the *Zitterbewegung* disappears if the negative energy states are neglected, and thus it is not supported in the nonrelativistic models, such as the standard Schrödinger equation and Pauli equation for nonrelativistic quantum particles. The *Zitterbewegung* effect is still debated and has not yet been observed in experiments.

IV. NONLINEAR ELECTROMAGNETIC WAVE PROPAGATION AND SELF-INDUCED TRANSPARENCY

It is well known [37] that a large-amplitude EM wave propagating in a classical plasma changes the dispersion properties of the plasma due to the relativistic mass increase of the electrons. We show here that the same effect occurs in our Klein-Gordon-Maxwell system.

We consider for simplicity the propagation of a circularly polarized electromagnetic (CPEM) wave of the form $\mathbf{A} = A_0[\widehat{\mathbf{x}}\cos(k_0 z - \omega_0 t) - \widehat{\mathbf{y}}\sin(k_0 z - \omega_0 t)]$, where ω_0 is the wave frequency and k_0 the wavenumber. Due to the circular polarization, the oscillatory parts in the nonlinear term proportional to A^2 in the Klein-Gordon equation vanish. Assuming that ψ depends only on time and not on space, and that $\phi = 0$, we obtain from Eq. (6)

$$\hbar^2 \frac{\partial^2 \psi}{\partial t^2} + m_e^2 c^4 \gamma_A^2 \psi = 0, \tag{25}$$

where $\gamma_A = \sqrt{1 + e^2 A_0^2/m_e^2 c^2}$ can be interpreted as the relativistic gamma factor due to the electron mass increase in the CPEM wave field. Equation (25) has the solution

$$\psi = \psi_0 \exp(-i m_e c^2 \gamma_A t/\hbar), \tag{26}$$

where the constant ψ_0 is determined by assuming the constant density $\rho_e = -en_0$ in Eq. (9).

Inserting (26) into (9) with $\rho_e = -en_0$, we obtain

$$|\psi_0|^2 = \frac{n_0}{\gamma_A}. \tag{27}$$

On the other hand, inserting (26) into (10) we have

$$\mathbf{j}_e = -\frac{e^2|\psi_0|^2}{m_e}\mathbf{A} = -\frac{e^2 n_0}{\gamma_A m_e}\mathbf{A}, \tag{28}$$

which can be inserted into (13) to obtain

$$\frac{1}{c^2}\frac{\partial^2 \mathbf{A}}{\partial t^2} - \nabla^2 \mathbf{A} = -\frac{\mu_0 e^2 n_0}{\gamma_A m_e}\mathbf{A}. \tag{29}$$

Equation (29) admits the nonlinear dispersion relation

$$\omega_0^2 = c^2 k^2 + \frac{\omega_{pe}^2}{\gamma_A}, \tag{30}$$

which predicts a relativistic downshift of the CPEM wave frequency due to relativistic electron mass increase in the CPEM wave field. Since the effective plasma frequency is decreased by a factor $1/\sqrt{\gamma_A}$, the model predicts the well-known self-induced transparency where the CPEM wave can propagate at frequencies below the electron plasma frequency. This is identical to the case of classical plasmas [37].

V. STIMULATED RAMAN SCATTERING AND MODULATIONAL INSTABILITIES

We now consider the instability of an intense CPEM wave in the quantum regime. In the presence of intense EM waves, we have the relativistic downshift in the EM wave frequency, given in (30), as well as possibility of exciting electrostatic oscillations via the parametric instabilities. As an example, we will here consider stimulated Raman scattering instability, in which an intense EM wave decays into a daughter EM wave and an electron plasma wave. The two-plasmon decay instability, in which the CPEM wave decays into two ES waves, will be treated elsewhere.

It is convenient to first introduce the transformation $\psi = \widetilde{\psi}\exp(-i\gamma_A m_e c^2 t/\hbar)$, where $\gamma_A = \sqrt{1 + e^2 A_0^2/m_e^2 c^2}$ and A_0 is the amplitude of the EM carrier wave $\mathbf{A}_0$. The wavefunction $\widetilde{\psi}$ obeys the modified KGE

$$\left(i\hbar\frac{\partial}{\partial t} + \gamma_A m_e c^2 + e\phi\right)^2 \widetilde{\psi} - c^2(-i\hbar\nabla + e\mathbf{A})^2\widetilde{\psi} - m_e^2 c^4 \widetilde{\psi} = 0, \tag{31}$$

and the electron charge density is given by

$$\rho_e = -\frac{i\hbar e}{2m_e c^2}\left(\widetilde{\psi}^*\frac{\partial \psi}{\partial t} - \psi\frac{\partial \widetilde{\psi}^*}{\partial t}\right) - \left(\gamma_A + \frac{e\phi}{m_e c^2}\right)e|\widetilde{\psi}|^2. \tag{32}$$

Let us now linearize our system of equations by introducing $\widetilde{\psi}(\mathbf{r},t) = \widetilde{\psi}_0 + \widetilde{\psi}_1(\mathbf{r},t)$ (where $\widetilde{\psi}_0$ is assumed to be constant), $\mathbf{A} = \mathbf{A}_0(\mathbf{r},t) + \mathbf{A}_1(\mathbf{r},t)$, and $\phi(\mathbf{r},t) = \phi_1(\mathbf{r},t)$. By using $\rho_i = en_0$ into Eq. (14), we note that the equilibrium quasineutrality requires that $\widetilde{\psi}_0$ is normalized such that $|\widetilde{\psi}_0|^2 = n_0/\gamma_A$. Supposing that $\mathbf{A}_0$ fulfills the plane wave equation (29), the linearized KGE (31), Poisson's equation (14), and the EM wave equation (16) then become, respectively,

$$\hbar^2\left(-\frac{\partial^2 \widetilde{\psi}_1}{\partial t^2} + c^2\nabla^2\widetilde{\psi}_1\right) + 2i\hbar\gamma_A m_e c^2\frac{\partial \widetilde{\psi}}{\partial t} + 2i\hbar c^2 e\mathbf{A}_0\cdot\nabla\widetilde{\psi}_1 + \left(2\gamma_A m_e c^2 e\phi_1 + i\hbar e\frac{\partial \phi_1}{\partial t}\right)\widetilde{\psi}_0 - 2c^2 e^2\mathbf{A}_0\cdot\mathbf{A}_1\widetilde{\psi}_0 = 0, \tag{33}$$

$$\nabla^2\phi_1 = \frac{ie\hbar}{2\varepsilon_0 m_e c^2}\left(\widetilde{\psi}_0^*\frac{\partial \widetilde{\psi}_1}{\partial t} - \widetilde{\psi}_0\frac{\partial \widetilde{\psi}_1^*}{\partial t}\right) + \frac{e\gamma_A}{\varepsilon_0}(\widetilde{\psi}_0^*\widetilde{\psi}_1 + \widetilde{\psi}_0\widetilde{\psi}_1^*) + \frac{\omega_{pe}^2}{\gamma_A c^2}\phi_1, \tag{34}$$

and

$$\nabla^2\left(\frac{\partial^2\mathbf{A}_1}{\partial t^2}-c^2\nabla^2\mathbf{A}_1+\frac{\omega_{pe}^2}{\gamma_A}\mathbf{A}_1\right)=\frac{\omega_{pe}^2}{n_0}\nabla\times\{\nabla\times[\mathbf{A}_0(\tilde{\psi}_0^*\tilde{\psi}_1+\tilde{\psi}_0\tilde{\psi}_1^*)]\}. \quad (35)$$

We note that the term proportional to $\mathbf{A}_0\cdot\nabla\tilde{\psi}_1$ in Eq. (33) gives rise to the two-plasmon decay, which we, however, do not consider here.

We now introduce the Fourier representations $\tilde{\psi}=\hat{\psi}_+\exp(-i\Omega t+i\mathbf{K}\cdot\mathbf{r})+\hat{\psi}_-\exp(i\Omega t-i\mathbf{K}\cdot\mathbf{r})$, $\phi_1=\hat{\phi}\exp(-i\Omega t+i\mathbf{K}\cdot\mathbf{r})+$ c.c., $\mathbf{A}_0=(1/2)\hat{\mathbf{A}}_0\exp(-\omega_0 t+\mathbf{k}_0\cdot\mathbf{r})+$ c.c., and $\mathbf{A}_1=[\hat{\mathbf{A}}_+\exp(-i\omega_+ t+i\mathbf{k}_+\cdot\mathbf{r})+\hat{\mathbf{A}}_-\exp(-i\omega_- t+i\mathbf{k}_-\cdot\mathbf{r})]+$ c.c., where we introduced $\omega_\pm=\omega_0\pm\Omega$ and $\mathbf{k}_\pm=\mathbf{k}_0\pm\mathbf{K}$, and c.c. stands for the complex conjugate. In one of the steps, we take the scalar product of both sides of the EM wave equation by $\hat{\mathbf{A}}_0^*$ and use the fact that $\hat{\mathbf{A}}_0^*\cdot[\mathbf{k}_\pm\times(\mathbf{k}_\pm\times\hat{\mathbf{A}}_0)]=(\mathbf{k}_\pm\times\hat{\mathbf{A}}_0)\cdot(\hat{\mathbf{A}}_0^*\times\mathbf{k}_\pm)=-|\mathbf{k}_\pm\times\hat{\mathbf{A}}_0|^2$. Separating different Fourier modes and eliminating the Fourier coefficients, we readily obtain the nonlinear dispersion relation

$$1+\frac{1}{\tilde{\chi}_e}=\frac{(c^2K^2-\Omega^2+\omega_{pe}^2/\gamma_A)}{\left[4\gamma_A^2m_e^2c^4-\hbar^2(\Omega^2-c^2K^2)\right]}\times\left[\frac{c^2e^2|\mathbf{k}_+\times\hat{\mathbf{A}}_0|^2}{k_+^2D_A(\omega_+,\mathbf{k}_+)}+\frac{c^2e^2|\mathbf{k}_-\times\hat{\mathbf{A}}_0|^2}{k_-^2D_A(\omega_-,\mathbf{k}_-)}\right], \quad (36)$$

where the EM sidebands are governed by $D_A(\omega_\pm,\mathbf{k}_\pm)=c^2k_\pm^2-\omega_\pm^2+\omega_{pe}^2/\gamma_A$. The electric susceptibility in the presence of the EM field is given by

$$\tilde{\chi}_e=\frac{\omega_{pe}^2\left[4\gamma_A^2m_e^2c^4-\hbar^2(\Omega^2-c^2K^2)\right]}{\gamma_A\left[\hbar^2(\Omega^2-c^2K^2)^2-4\gamma_A^2m_e^2c^4\Omega^2\right]}. \quad (37)$$

After reordering of terms, the nonlinear dispersion relation (36) can be written as

$$1-\frac{\omega_{pe}^2}{4\gamma_A^3m_e^2c^2}\frac{\left(c^2K^2-\Omega^2+\omega_{pe}^2/\gamma_A\right)}{\tilde{D}_L(\Omega,\mathbf{K})}\times\left[\frac{e^2|\mathbf{k}_+\times\hat{\mathbf{A}}_0|^2}{k_+^2D_A(\omega_+,\mathbf{k}_+)}+\frac{e^2|\mathbf{k}_-\times\hat{\mathbf{A}}_0|^2}{k_-^2D_A(\omega_-,\mathbf{k}_-)}\right]=0, \quad (38)$$

where the electron plasma oscillations in the presence of the EM field are represented by

$$\tilde{D}_L(\Omega,\mathbf{K})=\frac{\omega_{pe}^2}{\gamma_A}-\Omega^2+\frac{\hbar^2(\Omega^2-c^2K^2)}{4\gamma_A^2m_e^2c^4}\times\left(\Omega^2-c^2K^2-\frac{\omega_{pe}^2}{\gamma_A}\right). \quad (39)$$

We note that $D_L=0$ gives the dispersion relation for pure ES oscillations in the presence of a large-amplitude EM wave.

In the classical limit $\hbar\to 0$, we have $\tilde{\chi}_e=-\omega_{pe}^2/\Omega^2\gamma_A$, and the nonlinear dispersion relation takes the form

$$1-\frac{\Omega^2\gamma_A}{\omega_{pe}^2}=\frac{\left(c^2K^2-\Omega^2+\omega_{pe}^2/\gamma_A\right)}{4\gamma_A^2m_e^2c^2}\times\left[\frac{e^2|\mathbf{k}_+\times\hat{\mathbf{A}}_0|^2}{k_+^2D_A(\omega_+,\mathbf{k}_+)}+\frac{e^2|\mathbf{k}_-\times\hat{\mathbf{A}}_0|^2}{k_-^2D_A(\omega_-,\mathbf{k}_-)}\right], \quad (40)$$

which can be written in a more familiar form as

$$1-\left(\frac{c^2K^2}{D_L}+1\right)\frac{\omega_{pe}^2}{4\gamma_A^3m_e^2c^2}\times\left[\frac{e^2|\mathbf{k}_+\times\hat{\mathbf{A}}_0|^2}{k_+^2D_A(\omega_+,\mathbf{k}_+)}+\frac{e^2|\mathbf{k}_-\times\hat{\mathbf{A}}_0|^2}{k_-^2D_A(\omega_-,\mathbf{k}_-)}\right]=0, \quad (41)$$

with $D_L=\omega_{pe}^2/\gamma_A-\Omega^2$. These results can be compared with, for example, the dispersion relations obtained in Refs. [13,14,16] for the relativistic classical case and in Ref. [6] for the nonrelativistic classical case.

To proceed with the numerical evaluation of the nonlinear dispersion relation, we choose a coordinate system such that the CPEM takes the form $\hat{\mathbf{A}}_0=(\hat{\mathbf{x}}+i\hat{\mathbf{y}})\hat{A}_0$ and $\mathbf{k}_0=k_0\hat{\mathbf{z}}$. Without loss of generality, we choose $\mathbf{K}=K_{||}\hat{\mathbf{z}}+K_\perp\hat{\mathbf{y}}$. Then we have $K^2=K_{||}^2+K_\perp^2$, $\gamma_A=\sqrt{1+e^2|\hat{A}_0|^2/m_e^2c^2}$, $|\mathbf{k}_\pm\times\hat{\mathbf{A}}_0|^2=[2(k_0\pm K_{||})^2+K_\perp^2]|\hat{A}_0|^2$, and $k_\pm^2=(k_0\pm K_{||})^2+K_\perp^2$. We also use the fact that the carrier wave $\mathbf{A}_0$ obeys the nonlinear dispersion relation $\omega_0=\sqrt{c^2k_0^2+\omega_{pe}^2/\gamma_A}$.

We now assume that the wave frequency is complex valued, $\Omega=\Omega_R+i\Omega_I$, where Ω_R is the real frequency and Ω_I the growth rate, and solve numerically the dispersion relation (38) for Ω. In Fig. 2 we have plotted the growth rate for stimulated Raman scattering instability as a function of the wavenumbers $K_{||}$ and $K_\perp$, for a few values of $a_0=e|\hat{A}_0|/m_ec$ and $H=\hbar\omega_{pe}/m_ec^2$. For all cases in Fig. 2, we used $k_0c/\omega_{pe}=20$, which corresponds to a wavelength of 1.25×10^{-9} m for $H=10^{-4}$ and to 1.7×10^{-11} m for $H=0.007$, which is in the x-ray regime. We observe that for $H=10^{-4}$, there is a broad spectrum of unstable waves, in particular for $a_0=5$ and 10. For $H=0.007$, we observe a reduction in the spectrum of unstable waves and the growth rate (relative to the electron plasma frequency) is slightly reduced. This is due to the fact that the wavelength of unstable ES oscillations approaches the critical wavelength, where quantum dispersion effects become important compared to the plasma frequency. For $H=10^{-4}$, this wavelength is $\lambda_{\rm crit}=2\pi/(4\pi n_0/a_B)^{1/4}\approx5\times10^{-10}$ m, corresponding to a critical wavenumber $K_{\rm crit}=1.25\times10^{10}\,{\rm m}^{-1}$, and for $H=0.007$, we have $\lambda_{\rm crit}=2\pi/(4\pi n_0a_B)\approx2.8\times10^{-11}$ m, corresponding

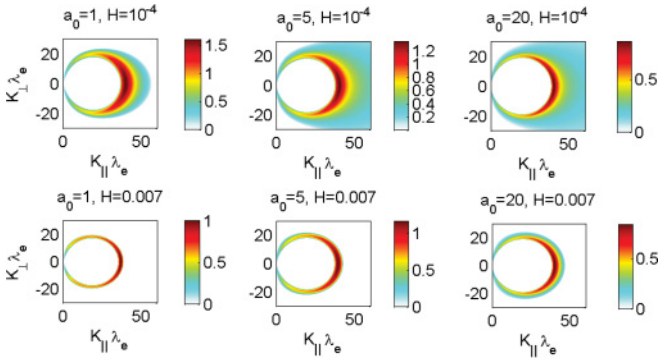

FIG. 2. (Color online) Growth rate (Ω_I/ω_{pe} vs. $K_{||}$ and $K_\perp$) for stimulated Raman scattering in the presence of a large-amplitude CPEM wave, for the amplitudes $a_0=1$, $a_0=5$, and $a_0=20$ (left to right panels) where $a_0=e|\hat{A}_0|/m_ec$ for $H=10^{-4}$ (top panels) and $H=0.007$ (bottom panels).

to $K_{\rm crit} = 2.25 \times 10^{11}$ m^{-1}. Hence, for $H = 0.007$ we have $k_0 \approx K_{\rm crit}$, which leads to the reduction of the growth rate due to the quantum dispersion effect.

Furthermore, it should be mentioned that we do not find Raman-type instabilities involving the pair branches in Fig. 1. This is consistent from the point of view of the conservation of charges, since the production of positrons would violate the conservation of electric charges.

In addition to stimulated Raman scattering instabilities, we also have the modulational instability that dominates for pump frequencies $\omega_0 < 2\omega_{pe}/\sqrt{\gamma_A}$ and the corresponding wavenumbers $k_0 < (\omega_{pe}/c)\sqrt{3/\gamma_A}$. The modulational instability usually occurs for small modulation wavenumbers and saturates nonlinearly by the formation of relatively small localized structures and solitary waves. In the past, such nonlinear structures have been studied for classical plasmas in one [38] and three dimensions [39]. We have investigated the modulational instability for the CPEM dipole field with $k_0 = 0$ and have plotted the results in Fig. 3 for different amplitudes :$a_0 = 1$, $a_0 = 5$, and $a_0 = 20$. We find that the growth rate is relatively insensitive to the quantum parameter H. We have used $H = 0.007$ in Fig. 3, but $H = 0$ gives almost identical results. This is understandable since the modulational instability takes place on relatively large scales, and the quantum effect is thus negligible. However, we will investigate the quantum effect on the relatively small-scale nonlinear structures below.

VI. RELATIVISTIC OPTICAL SOLITARY WAVES

Here we illustrate the existence of large-amplitude localized CPEM wave excitations at the quantum scale in our system. We restrict our investigation to one-space dimension, which has also been studied for classical plasmas [38].

Far from the local excitation, one can assume that the dynamics of the plasma is nonrelativistic. To shorten the algebraic steps, it is convenient first to introduce a new wavefunction $\widetilde{\psi}(z,t)$ and the potential Φ via the transformations $\psi(\mathbf{r},t) = \widetilde{\psi}(z,t)\exp(-im_ec^2t/\hbar)$ and $\phi = \Phi - m_ec^2/e$, and which satisfy the KGE

$$\left(i\hbar\frac{\partial}{\partial t} + e\Phi\right)^2\widetilde{\psi} + \hbar^2c^2\frac{\partial^2\widetilde{\psi}}{\partial z^2} - \gamma_A^2m_e^2c^4\widetilde{\psi} = 0, \quad (42)$$

where $\gamma_A = (1 + e^2A^2/m_e^2c^2)^{1/2}$. In this gauge, the wavefunction $\widetilde{\psi}$ is nonoscillatory in time, and the new potential takes

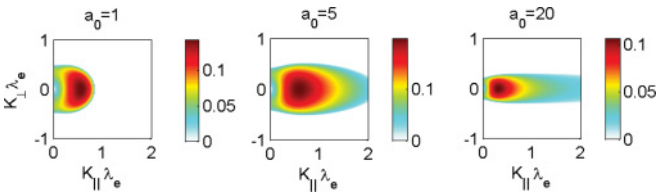

FIG. 3. (Color online) The growth rate (Ω_I/ω_{pe} vs. $K_{||}$ and $K_\perp$) for the modulational instability in the presence of a large-amplitude CPEM wave, for the amplitudes $a_0 = 1$ (left panel), $a_0 = 5$ (middle panel), and $a_0 = 20$ (right panel) where $a_0 = e|\widehat{A}_0|/m_ec$. $H = 0.007$ for all cases.

the value $\Phi = e/m_ec^2$, far from the solitary wave where the plasma is at rest. The electron charge density is expressed as

$$\rho_e = -\frac{e}{m_ec^2}\left[\frac{i\hbar}{2}\left(\widetilde{\psi}^*\frac{\partial\widetilde{\psi}}{\partial t} - \widetilde{\psi}\frac{\partial\widetilde{\psi}^*}{\partial t}\right) + e\Phi|\widetilde{\psi}|^2\right]. \quad (43)$$

We now study quasi-steady-state structures propagating with a constant speed v_0, so that $\phi = \phi(\xi)$ and $A^2 = A^2(\xi)$, where $\xi = z - v_0t$ and $A^2 = |\mathbf{A}|^2$. The CPEM wavevector potential is of the form $\mathbf{A} = A(\xi)[\widehat{\mathbf{x}}\cos(k_0z - \omega_0t) - \widehat{\mathbf{y}}\sin(k_0z - \omega_0t)]$. It is convenient to introduce the eikonal representation $\widetilde{\psi} = P(\xi)\exp[i\theta(\xi)]$, where P and θ are real valued. Then the KGE (42) takes the form

$$\begin{aligned}&\hbar^2(c^2 - v_0^2)\left[\frac{d^2P}{d\xi^2} - P\left(\frac{d\theta}{d\xi}\right)^2 + 2i\frac{dP}{d\xi}\frac{d\theta}{d\xi} + iP\frac{d^2\theta}{d\xi^2}\right]\\ &\quad - i\hbar ev_0\frac{d\Phi}{d\xi}P - 2i\hbar e\Phi v_0\left(\frac{dP}{d\xi} + iP\frac{d\theta}{d\xi}\right)\\ &\quad + \left(e^2\Phi^2 - m_e^2c^4\gamma_A^2\right)P = 0. \end{aligned} \quad (44)$$

Setting the imaginary part of Eq. (44) to zero, we obtain

$$2U\frac{dP}{d\xi} + P\frac{dU}{d\xi} = 0, \quad (45)$$

where

$$U = \hbar^2(c^2 - v_0^2)\frac{d\theta}{d\xi} - \hbar e\Phi v_0. \quad (46)$$

The solution of Eq. (45) is $P^2U = D =$ const. Using the boundary conditions $P^2 = n_0$, $\phi = 0$ (hence $\Phi = m_ec^2/e$), and $d/d\xi = 0$ at $|\xi| = \infty$, we have $D = -n_0\hbar m_ec^2v_0$. Hence, we obtain

$$\frac{d\theta}{d\xi} = \frac{v_0m_e\gamma_0^2}{\hbar}\left(\frac{e\Phi}{m_ec^2} - \frac{n_0}{P^2}\right), \quad (47)$$

where we have denoted

$$\gamma_0 = \frac{1}{\sqrt{1 - v_0^2/c^2}}. \quad (48)$$

The electron charge density (43) now takes the form

$$\rho_e = -\frac{e}{m_ec^2}\left(\hbar v_0\frac{d\theta}{d\xi} + e\Phi\right)P^2, \quad (49)$$

which, by using Eq. (47), can be written as

$$\rho_e = -en_0\gamma_0^2\left(-\frac{v_0^2}{c^2} + \frac{e\Phi}{m_ec^2}\frac{P^2}{n_0}\right), \quad (50)$$

and hence Poisson's equation (14), with $\rho_i = en_0$, becomes

$$\frac{d^2\Phi}{d\xi^2} = \frac{en_0\gamma_0^2}{\varepsilon_0}\left(\frac{e\Phi}{m_ec^2}\frac{P^2}{n_0} - 1\right). \quad (51)$$

On the other hand, by setting the real part of Eq. (44) to zero, we have

$$\begin{aligned}&\frac{\hbar^2c^2}{\gamma_0^2}\left[\frac{d^2P}{d\xi^2} - P\left(\frac{d\theta}{d\xi}\right)^2\right]\\ &\quad + 2\hbar e\Phi v_0P\frac{d\theta}{d\xi} + \left(e^2\Phi^2 - m_e^2c^4\gamma_A^2\right)P = 0, \end{aligned} \quad (52)$$

which, by using Eq. (47), can be written as

$$\hbar^2\frac{d^2P}{d\xi^2}+m_e^2c^2\gamma_0^4\left[\frac{e^2\Phi^2}{m_e^2c^4}-\frac{v_0^2}{c^2}\frac{n_0^2}{P^4}-\frac{\gamma_A^2}{\gamma_0^2}\right]P=0. \quad (53)$$

Finally, inserting the ansatz $\mathbf{A}=A(\xi)[\hat{\mathbf{x}}\cos(k_0z-\omega_0t)-\hat{\mathbf{y}}\sin(k_0z-\omega_0t)]$ for the vector potential, together with the current

$$\mathbf{j}_e=-\frac{e^2}{m_e}|\psi|^2\mathbf{A}=-\frac{e^2}{m_e}P^2\mathbf{A}, \quad (54)$$

into Eq. (16), we obtain the EM wave equation

$$\frac{d^2A}{d\xi^2}+\frac{\omega_{pe}^2}{c^2}\left[\lambda+\gamma_0^2\left(1-\frac{P^2}{n_0}\right)\right]A=0, \quad (55)$$

where we have used $k_0=\omega_0v_0/c^2$, and where $\lambda=(c^2/\omega_{pe}^2)(\omega_0^2-\omega_p^2-c^2k_0^2)/(c^2-v_0^2)=\omega_0^2/\omega_{pe}^2-\gamma_0^2$ is a nonlinear eigenvalue of the system that determines the wave frequency ω_0.

The coupled system (51), (53), and (55) describes the profile of EM solitary waves in a quantum plasma. It has the conserved quantity $\mathcal{H}=0$, where

$$\mathcal{H}=-\frac{c^2}{\omega_{pe}^2}\left(\frac{d}{d\xi}\frac{e\Phi}{m_ec^2}\right)^2+\frac{\hbar^2}{\gamma_0^2m_e^2c^2n_0}\left(\frac{dP}{d\xi}\right)^2+\frac{c^2}{\omega_{pe}^2\gamma_0^2}\times\left(\frac{d}{d\xi}\frac{eA}{m_ec}\right)^2+\left(\frac{\lambda}{\gamma_0^2}+1-\frac{P^2}{n_0}\right)\frac{e^2A^2}{m_e^2c^2}+\gamma_0^2\frac{e^2\Phi^2}{m_e^2c^4}\frac{P^2}{n_0}-2\gamma_0^2\frac{e\Phi}{m_ec^2}+\frac{v_0^2\gamma_0^2}{c^2}\left(\frac{n_0}{P^2}-1\right)-\frac{P^2}{n_0}+1+\gamma_0^2. \quad (56)$$

The conserved quantity $\mathcal{H}$ can be used to check that the numerical scheme used to solve the nonlinear system of Eqs. (51), (53), and (55) produces correct results.

In Fig. 4 we have compared the present model with our previous results in Ref. [40] where we used a simplified model to describe nonlinear interactions between intense CPEM wave and a quantum plasma. We used the same parameters as in Fig. 2 of Ref. [40], to produce the profiles of the CPEM wave potential, the electron charge density, and the ES potential. We observe that the present results are almost identical to our previous work [40]. For our sets of parameters, the quantum effect on the profiles of the EM solitary waves are small, and there is only a slight difference in the profiles of the electron density for the two values $H=0.002$ and 0.007. For standing EM solitary waves, such as the ones in Figs. 4(a) and 4(b), the solutions are localized with exponentially decaying tails. By linearizing the system of Eqs. (51), (53), and (55), one can show that far from the EM soliton, A decays as $\exp(\sqrt{-\lambda}\xi)$, while P and ϕ are proportional to $\exp(K\xi)$, where K is found from the dispersion relation

$$\hbar c^2K^2\left(c^2K^2+\gamma_0\omega_{pe}^2\right)-4\gamma_0^4m_e^2c^4\left(v_0^2K^2-\omega_{pe}^2\right)=0. \quad (57)$$

For $v_0=0$ (and $\gamma_0=1$), we see immediately that there exist only complex-valued K, which means that the quasi-stationary-wave solutions decay exponentially far away from the EM solitary wave. However, in the classical limit $\hbar\to0$, we instead have the plasma wake oscillations given by real-valued $K=\omega_{pe}/v_0$. Hence, a localized EM pulse will create an oscillatory wake that extends far from the EM pulse. In one-space dimension, there also exist special classes of propagating

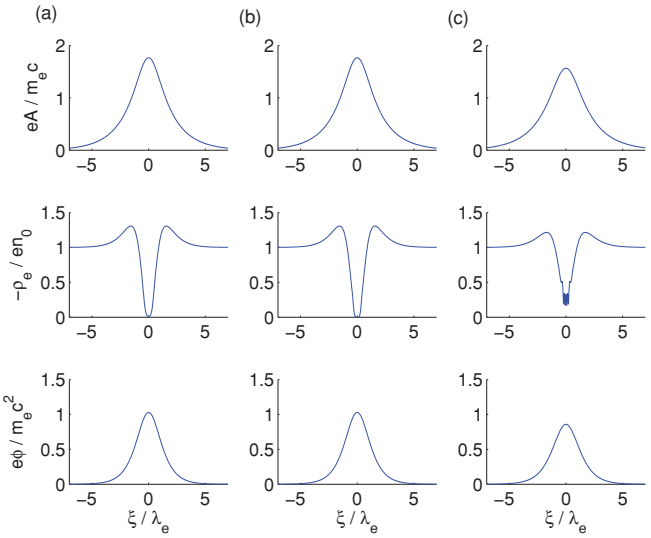

FIG. 4. (Color online) The spatial profiles of the vector potential, the electron charge density, and the electrostatic potential (top to bottom panels), for standing solitary waves ($v_0=0$) for (a) $H=0.007$ and $\lambda=-0.34$, (b) $H=0.002$ and $\lambda=-0.34$, and (c) for a moving solitary wave with $v_0=0.0059c$ for $H=0.002$ and $\lambda=-0.30$.

localized EM envelope solutions [41,42]. In addition to the wake oscillations, we also have quantum oscillations in quantum plasmas. In Fig. 4(c), we show an example of a slowly moving envelope EM soliton, where small-scale oscillations in the charge density are clearly visible.

We note that the cold fluid results can be retained in the classical limit $\hbar\to0$. Then Eq. (53) can be written as

$$\frac{e^2\Phi^2}{m_e^2c^4}=\frac{v_0^2}{c^2}\frac{n_0^2}{P^4}+\frac{\gamma_A^2}{\gamma_0^2}. \quad (58)$$

By setting $\rho_e=-en_e$, where n_e is the electron number density, in Eq. (50) and solving for P, we obtain

$$\frac{P^2}{n_0}=\left[1+\frac{1}{\gamma_0^2}\left(\frac{n_e}{n_0}-1\right)\right]\frac{m_ec^2}{e\Phi}, \quad (59)$$

which can be inserted into (58) to obtain

$$\left[\frac{1}{\gamma_0^2}\frac{n_e}{n_0}+\frac{v_0^2}{c^2}\right]\Big/\left[\frac{n_e^2}{n_0^2}-\frac{v_0^2}{c^2}\left(\frac{n_e}{n_0}-1\right)^2\right]^{1/2}=\frac{e\Phi}{\gamma_Am_ec^2}, \quad (60)$$

which relates n_e to Φ and γ_A at a given speed v_0. The relation (60) can also be obtained from the cold electron fluid model [41] and hence confirms the classical limit of the quantum model used here. If, furthermore, we assume standing waves such that $v_0=0$, then we have from (60)

$$\frac{e\Phi}{m_ec^2}=\gamma_A. \quad (61)$$

Solving for Φ and inserting the result into Poisson's equation (51), we have

$$\lambda_e^2\frac{d^2\gamma_A}{d\xi^2}=\gamma_A\frac{P^2}{n_0}-1. \quad (62)$$

Finally, solving for P^2 and inserting the result into Eq. (55), we obtain

$$\lambda_e^2\frac{d^2A}{d\xi^2}+\frac{\omega_0^2}{\omega_p^2}A=\left(\lambda_e^2\frac{d^2\gamma_A}{d\xi^2}+1\right)\frac{A}{\gamma_A}, \tag{63}$$

where we have used $v_0=0$ and, therefore, $k_0=0$. Equation (63) is identical to the model of Marburger and Tooper [38] for the nonlinear optical standing wave in a classical cold fluid electron plasma. The relativistic mass increase is reflected by the ratio A/γ_A in the right-hand side of Eq. (63). The nonlinear electron density fluctuations, which are reflected in the term proportional to $d^2\gamma_A/d\xi^2$ in the right-hand side of Eq. (63) can often be neglected in the weakly relativistic case [43].

We note that our previous model [40] can be recovered in the weakly relativistic limit, in the following manner. Assuming that, to first order, we have a balance between the ponderomotive and electrostatic pressures, so that $1+e\phi/m_ec^2\approx\gamma_A$ and that $\gamma_A\approx 1$, with $v_0^2\ll c^2$. Accordingly, we have

$$\hbar^2c^2\frac{d^2P}{d\xi^2}+2m_e^2c^4\left(1+\frac{e\phi}{m_ec^2}-\gamma_A\right)P=0, \tag{64}$$

Poisson's equation

$$\frac{d^2\phi}{d\xi^2}=\frac{en_0}{\varepsilon_0}\left(\frac{\gamma_AP}{n_0}-1\right), \tag{65}$$

and the CPEM wave equation

$$\frac{d^2A}{d\xi^2}+\lambda A=\frac{\omega_{pe}^2}{c^2}\left(\frac{P^2}{n_0}-1\right)A. \tag{66}$$

We now make a simple change of variables $\gamma_AP=\widetilde{P}$. Then we have, by neglecting terms containing $d\gamma_A/d\xi$, the model [40]

$$\hbar^2c^2\frac{d^2\widetilde{P}}{d\xi^2}+2m_e^2c^4\left(1+\frac{e\phi}{m_ec^2}-\gamma_A\right)\widetilde{P}=0, \tag{67}$$

$$\frac{d^2\phi}{d\xi^2}=\frac{en_0}{\varepsilon_0}\left(\frac{\widetilde{P}}{n_0}-1\right), \tag{68}$$

and

$$\frac{d^2A}{d\xi^2}+\lambda A=\frac{\omega_{pe}^2}{c^2}\left(\frac{\widetilde{P}^2}{\gamma_An_0}-1\right)A, \tag{69}$$

where the relativistic mass increase appears explicitly in the CPEM wave equation.

VII. DYNAMICS OF NONLINEARLY INTERACTING EM WAVES IN A QUANTUM PLASMA

In order to study the dynamics of nonlinear interactions between intense CPEM waves and a quantum plasma, we have carried out numerical simulations of the Klein-Gordon-Maxwell system of equations. We have here restricted our study to one-space dimension, along the z direction in space, and written our governing equations in the form

$$\left(i\hbar\frac{\partial}{\partial t}+e\phi\right)\psi=W, \tag{70}$$

$$\left(i\hbar\frac{\partial}{\partial t}+e\phi\right)W+\hbar^2c^2\frac{\partial^2\psi}{\partial z^2}-\gamma_A^2m_e^2c^4\psi=0, \tag{71}$$

$$\frac{1}{c^2}\frac{\partial^2\mathbf{A}}{\partial t^2}-\frac{\partial^2\mathbf{A}}{\partial z^2}=-\frac{\mu_0e^2}{m_e}|\psi|^2\mathbf{A}, \tag{72}$$

and

$$\frac{\partial^2\phi}{\partial z^2}=\frac{e}{2m_ec^2\varepsilon_0}(\psi^*W+\psi W^*)-\frac{en_0}{\varepsilon_0}. \tag{73}$$

We have used a periodic simulation box in space, of length $L_x=63\ \lambda_e$ and used of the order 10^4 grid points to resolve the solution in space. It is important to resolve the relatively long electron skin depth scale as well as the shorter length scale associated with accelerated electrons with the momentum $p=\hbar k$ and the associated wavelength $\lambda=2\pi/k=2\pi\hbar/p$. Since we need at least two grid points per wavelength to represent the solution, the required grid size is $\Delta x<\pi\hbar/p$, which can be written $\Delta x/\lambda_e<\pi Hm_ec/p$. For example, to represent the wavefunction of relativistic electrons with the momentum $p=m_ec$, we need a spatial grid with $\Delta x/\lambda_e<\pi H\approx 0.022$ to represent the wavefunction for $H=0.007$. The solution was advanced in time with the standard fourth-order Runge-Kutta scheme, using a time step of order $\Delta t=10^{-4}\ \omega_{pe}$.

We first numerically study the growth and nonlinear saturation of the modulational instability, which is relevant for dense matters where the plasma is overdense or close to overdense. As initial conditions, we used a CPEM pump wave of the form $\mathbf{A}=A_0[\hat{\mathbf{x}}\cos(k_0z)-\hat{\mathbf{y}}\sin(k_0z)]$ with $k_0=0$ and $A_0/m_ec=1$. A small amplitude noise (random numbers) was added to A in order to seed any instability in the system. As initial conditions for the wavefunction, we used $\psi=\sqrt{n_0/\gamma_A}$ and $W=m_ec^2\sqrt{n_0\gamma_A}$, corresponding to a pure electronic state at equilibrium. The initially homogeneous electron density was set to $n_e=n_0=10^{30}\ \mathrm{m}^{-3}$, corresponding to $H=0.007$ [cf. Eq. (24)]. In this situation, the EM wave is unstable due to the modulational instability, which has instability for small wavenumbers, as shown in Fig. 3. In the nonlinear stage, we see in Fig. 5 that the CEPM wave envelope has been focused into localized wavepackets similar to the ones in Fig. 4, associated with depletions in the electron density and positive electrostatic potentials. The collapse of the CPEM wave packet leads to relativistically strong ponderomotive potentials that accelerate electrons to relativistic speeds. The relativistic electrons are associated with small-scale spatial oscillations in the wavefunction, where the wavelength is comparable to or even smaller than the Compton wavelength. In order to study the distribution of electrons both in space and momentum space, we have performed a Fourier transform of the wavefunction ψ using a moving window technique (using a Hann window) in space. The width of the window has been tuned so that it provides a good resolution both in space and in momentum space. The resulting spatial spectrogram gives a representation of the distribution of the electrons both in space and in momentum space; see Fig. 5(d), where the color indicates the density of electrons in phase space. In Fig. 6(d) the horizontal axis shows the spatial dependence, and the vertical axis shows the momentum dependence via the relation $p=\hbar k$ between the momentum p and the wavenumber k. In this figure it is clear that in the collapse stage of the solitary waves, bunches of electrons are accelerated to relativistic speeds and form self-trapped, Bernstein-Greene-Kruskal (BGK) -like

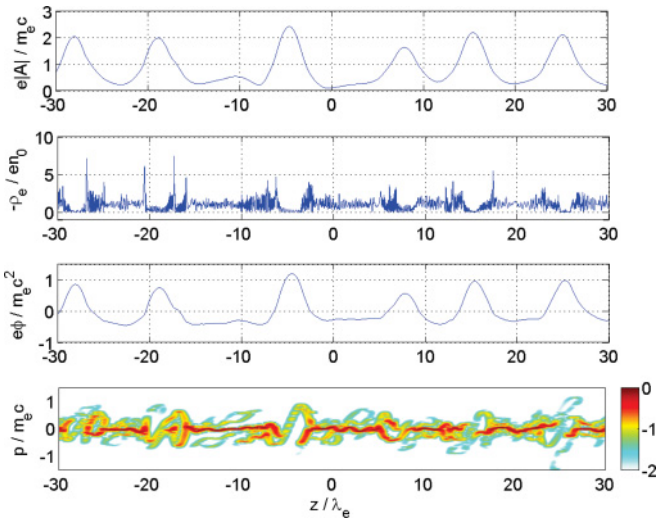

FIG. 5. (Color online) The nonlinear stage of a modulational instability, showing localized EM wave-packets associated with depletions in the electron charge density, and positive ES potentials. The electron pseudodistribution function shows that the electrons have been accelerated and form BGK-like modes that travel away from the collapsed wave packets. Parameters are $H = 0.007$ and initially a dipole field $a_0 = 1$ with $k_0 = 0$.

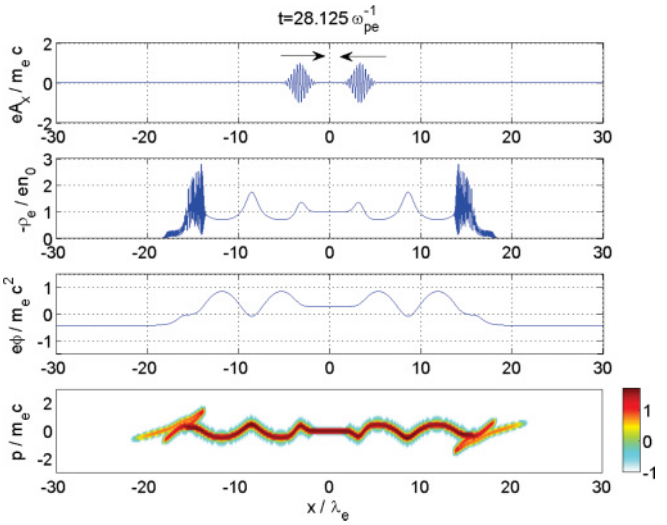

FIG. 6. (Color online) Attosecond laser pulse propagation into an underdense quantum plasma, at time $t = 28.125\ \omega_{pe}^{-1}$. Top to bottom panels show (a) the vector potential of the EM pulse (the arrows show the propagation directions of the pulses), (b) the electron charge density, (c) the ES potential, and (d) the distribution of electrons in phase space in a 10-logarithmic color scale. Parameters are $H = 0.007$, amplitude $a_0 = 1$ and wavenumber $k_0 = 20\ \lambda_e^{-1}$. Localized EM pulses excite large-amplitude oscillatory potential wakes behind them, as they penetrate the plasma slab.

modes that propagate away from the collapsed EM wave packets.

Next, we investigate a scenario of the short EM pulse propagation and the wake-field generation in a quantum plasma. This concept is traditionally used for electron acceleration in classical plasmas [44,45]. The numerical results are displayed in Figs. 6 and 7. Here two attosecond pulses are injected from each side of a plasma slab and are allowed to collide at the center of the slab. As initial conditions, we used a CPEM pump wave of the form $\mathbf{A} = A_0(z)[\widehat{\mathbf{x}}\cos(k_0 z) - \widehat{\mathbf{y}}\sin(k_0 z)]$ with $k_0 = 20\ \lambda_e^{-1}$ and envelopes of the form $A_0(z)/m_e c = \exp(-(z/\lambda_e \pm 30)^2)$ propagating into the plasma slab. The plasma slab is initially centered between $z = \pm 15\lambda_e$ with equal electrons with the number densities n_0, where the electron wavefunction was set to $\psi = \sqrt{n_0}$ and $W = m_e c^2\sqrt{n_0}$. After a time $t = 28.125\ \omega_{pe}^{-1}$, we see in Fig. 6(b) and 6(c) that the large-amplitude CPEM pulses excite plasma wake oscillations associated with large-amplitude positive potentials, and with an approximate wavelength of $2\pi c/\omega_{pe}$, corresponding to a leading wavenumber of ω_{pe}/c. The positive potentials of the plasma wake oscillations are starting to capture populations of the electrons at edges of the plasma slab, at $x \approx \pm 15\lambda_e$. A high-frequency diffraction pattern is formed in the electron density, as faster electrons overtake slower electrons. Later, at $t = 37.5\ \omega_{pe}^{-1}$, the two EM pulses have collided and passed through each other. Trapped electrons have been further accelerated to ultrarelativistic speeds, as seen in Fig. 7(d) at $x \approx \pm 5\lambda_e$., where the fastest electrons have reached a momentum of $\approx 5\ m_e c$.

VIII. SUMMARY AND CONCLUSIONS

In this paper, we have developed a relativistic model for treating nonlinear interactions between intense EM waves and a quantum plasma. Our nonlinear model is based on the coupled Klein-Gordon and Maxwell equations for the relativistic electron momentum and the EM fields. In our fully relativistic nonlinear model, the electron current and charge densities are calculated self-consistently from the KGE, and they enter as sources for the nonlinear EM and ES waves in the Maxwell equation. The KG-Maxwell system of equations has been used to derive the linear dispersion relation for the ES and EM waves, as well as for investigating stimulated Raman scattering and modulational instabilities in the presence of relativistically

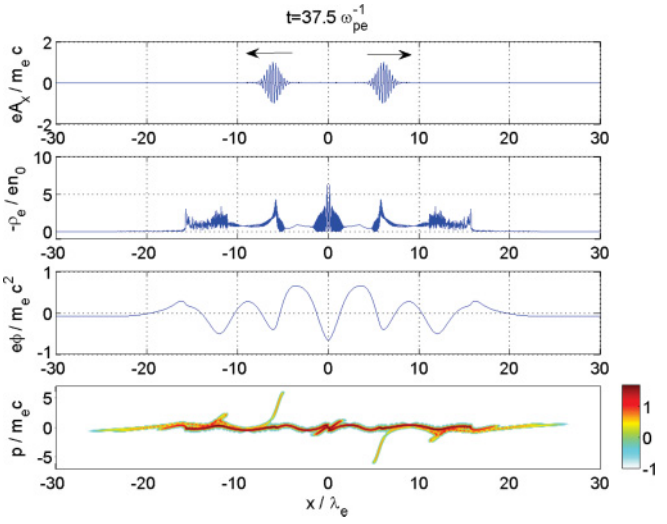

FIG. 7. (Color online) The same as in Fig. 6 at time $t = 37.5\ \omega_{pe}^{-1}$. Groups of electrons are accelerated to ultrarelativistic speeds by the large-amplitude ES wake field.

intense CPEM waves. In the linear regime, the general dispersion relation for the ES waves exhibits the quantum effect associated with the overlapping electron wavefunction. At long-wavelengths, we have the dispersive Langmuir oscillations with frequencies close to the electron plasma frequency, while at shorter wavelengths we have the oscillation frequency of free electrons. At wavelengths comparable to or larger than the Compton wavelength, the electron motion is fully relativistic. In the nonlinear regime, we have demonstrated the existence of fully relativistic stimulated Raman scattering and modulational instabilities. While the Raman amplification is of much interest for generating a coherent EM radiation, the modulational instability gives rise to the localization and collapse of the CPEM waves into localized solitary EM wave packets. Indeed, numerical simulations of the coupled KG-Maxwell equations reveal the collapse and acceleration of electrons in the nonlinear stage of the modulational instability, as well as possibility of wake-field acceleration of electrons to relativistic speeds by short EM pulses at nanometer scales. In conclusion, we stress that the present investigation of nonlinear effects dealing with intense EM wave interactions with a quantum plasma is relevant for the compression of x-ray free-electron EM pulses to attosecond duration [46,47], as well as to the understanding of localized intense x-ray and γ-ray bursts that emanate from compact astrophysical objects [29,30].

ACKNOWLEDGMENTS

This work was financially supported by the Swedish Research Council (VR).

[1] E. Hand, Nature (London) **461**, 708 (2009).
[2] S. H. Glenzer *et al.*, Phys. Rev. Lett. **98**, 065002 (2007); P. Neumayer *et al.*, *ibid.* **105**, 075003 (2010); S. H. Glenzer and R. Redmer, Rev. Mod. Phys. **81**, 1625 (2009).
[3] A. V. Andreev, JETP Lett. **72**, 238 (2000).
[4] G. Mourou *et al.*, Rev. Mod. Phys. **78**, 309 (2006).
[5] M. Marklund and P. K. Shukla, Rev. Mod. Phys. **78**, 591 (2006).
[6] J. F. Drake, P. K. Kaw, Y. C. Lee, G. Schmidt, C. S. Liu, and M. N. Rosenbluth, Phys. Fluids **17**, 778 (1974).
[7] R. P. Sharma and P. K. Shukla, Phys. Fluids **26**, 87 (1983).
[8] G. Murtaza and P. K. Shukla, J. Plasma Phys. **31**, 423 (1984).
[9] P. K. Shukla *et al.*, Phys. Rep. **138**, 1 (1986).
[10] C. J. McKinstrie and R. Bingham, Phys. Fluids B **1**, 230 (1989).
[11] L. N. Tsintsadze, Sov. J. Plasma Phys. **17**, 872 (1991).
[12] C. J. McKinstrie and R. Bingham, Phys. Fluids B **4**, 2626 (1992).
[13] A. S. Sakharov and V. I. Kirsanov, Phys. Rev. E **49**, 3274 (1994).
[14] S. Guérin, G. Laval, P. Mora, J. C. Adam, A. Héron, and A. Bendib, Phys. Plasmas **2**, 2807 (1995).
[15] J. C. Adam, A. Héron, G. Laval, and P. Mora, Phys. Rev. Lett. **84**, 3598 (2000).
[16] B. Quesnel, P. Mora, J. C. Adam, A. Héron, and G. Laval, Phys. Plasmas **4**, 3358 (1997).
[17] L. Stenflo, Phys. Scr. **14**, 320 (1976).
[18] L. Stenflo, Phys. Scr. **21**, 831 (1980).
[19] L. Stenflo and H. Wilhelmsson, Phys. Rev. A **24**, 1115 (1981).
[20] T. Takabayasi, Prog. Theor. Phys. **9**, 187 (1953).
[21] H. Feshbach and F. Villars, Rev. Mod. Phys. **30**, 24 (1958).
[22] D. F. Hines and N. E. Frankel, Phys. Lett. A **69**, 301 (1978).
[23] V. Kowalenko, N. E. Frankel, and K. C. Hines, Phys. Rep. **126**, 109 (1985).
[24] V. M. Malkin, N. J. Fisch, and J. S. Wurtele, Phys. Rev. E **75**, 026404 (2007).
[25] A. Serbeto *et al.*, Phys. Plasmas **15**, 013110 (2008).
[26] A. Serbeto, L. F. Monteiro, K. H. Tsui, and J. T. Mendonça, Plasma Phys. Controlled Fusion **51**, 124024 (2009).
[27] N. Piovella, M. M. Cola, L. Volpe, A. Schiavi, and R. Bonifacio, Phys. Rev. Lett. **100**, 044801 (2008).
[28] G. Chabrier *et al.*, J. Phys. Condens. Matter **14**, 9133 (2002); J. Phys. A: Math. Gen. **39**, 4411 (2006).
[29] M. J. Coe *et al.*, Nature (London) **272**, 37 (1978); D. K. Galloway and J. L. Sokoloski, Astrophys. J. **613**, L61 (2004).
[30] K. Hurley *et al.*, Nature (London) **434**, 1098 (2005); A. K. Harding and D. Lai, Rep. Prog. Phys. **69**, 2631 (2006).
[31] P. R. Holland, *The Quantum Theory of Motion: An Account of the De Broglie-Bohm Causal Interpretation of Quantum Mechanics* (Cambridge University Press, Cambridge, UK, 1993).
[32] M. Marklund and G. Brodin, Phys. Rev. Lett. **98**, 025001 (2007).
[33] G. Brodin, M. Marklund, and G. Manfredi, Phys. Rev. Lett. **100**, 175001 (2008).
[34] G. Manfredi and F. Haas, Phys. Rev. B **64**, 075316 (2001); P. K. Shukla and B. Eliasson, Phys. Rev. Lett. **96**, 245001 (2006); Phys. Usp. **53**, 51 (2010).
[35] M. G. Fuda and E. Furlani, Am. J. Phys. **50**, 545 (1982).
[36] R. Gerritsma *et al.*, Nature (London) **463**, 68 (2010).
[37] A. I. Akhiezer and R. V. Polovin, Sov. Phys. JETP **3**, 696 (1956); Zh. Eksp. Teor. Fiz. **30**, 915 (1956); P. Kaw and J. Dawson, Phys. Fluids **13**, 472 (1970); C. Max and F. Perkins, Phys. Rev. Lett. **27**, 1342 (1971).
[38] J. H. Marburger and R. F. Tooper, Phys. Rev. Lett. **35**, 1001 (1975).
[39] J. I. Gersten and N. Tzoar, Phys. Rev. Lett. **35**, 934 (1975).
[40] P. K. Shukla and B. Eliasson, Phys. Rev. Lett. **99**, 096401 (2007).
[41] P. K. Kaw, A. Sen, and T. Katsouleas, Phys. Rev. Lett. **68**, 3172 (1992).
[42] V. Saxena, A. Das, A. Sen, and P. Kaw, Phys. Plasmas **13**, 032309 (2006).
[43] P. K. Shukla, N. N. Rao, M. Y. Yu, and N. L. Tsintsadze, Phys. Rep. **138**, 1 (1986).
[44] T. Tajima and J. M. Dawson, Phys. Rev. Lett. **43**, 267 (1979).
[45] R. Bingham *et al.*, Plasma Phys. Controlled Fusion **46**, R1 (2004).
[46] P. M. Paul *et al.*, Science **292**, 1689 (2001).
[47] R. M. G. M. Trines *et al.*, Nature Phys. **6**, 1793 (2010).